

Article

Highly Reliable Short-Circuit Protection Circuits for Gallium Nitride High-Electron-Mobility Transistors

Chul-Min Kim, Hyun-Soo Yoon, Jong-Soo Kim  and Nam-Joon Kim *

Department of Electrical Engineering, Daejin University, Pocheon 11159, Republic of Korea; cmkim@daejin.ac.kr (C.-M.K.); ab223015@daejin.ac.kr (H.-S.Y.); jskim2@daejin.ac.kr (J.-S.K.)

* Correspondence: njkim@daejin.ac.kr

Abstract: This paper presents a circuit for detecting and protecting against short circuits in E-mode gallium nitride high-electron-mobility transistors (GaN HEMTs) and analyzes the protection performance of the circuit. GaN HEMTs possess fast switching characteristics that enable high efficiency and power density in power conversion devices. However, these characteristics also pose challenges in protecting against short circuits and overcurrent situations. The proposed method detects short-circuit events by monitoring an instantaneous drop in the DC bus voltage of a circuit with GaN HEMTs applied and uses a bandpass filter to prevent the malfunction of the short-circuit protection circuit during normal switching and ensure highly reliable operation. Using this method, the short-circuit detection time of E-mode GaN HEMTs can be reduced to 257 ns, successfully protecting the device without malfunctions even in severe short-circuit situations occurring at high DC link voltages.

Keywords: GaN HEMT; short-circuit protection; reliability



Citation: Kim, C.-M.; Yoon, H.-S.; Kim, J.-S.; Kim, N.-J. Highly Reliable Short-Circuit Protection Circuits for Gallium Nitride High-Electron-Mobility Transistors. *Electronics* **2024**, *13*, 1203. <https://doi.org/10.3390/electronics13071203>

Academic Editor: Francesco Giuseppe Della Corte

Received: 19 February 2024

Revised: 17 March 2024

Accepted: 22 March 2024

Published: 25 March 2024



Copyright: © 2024 by the authors. Licensee MDPI, Basel, Switzerland. This article is an open access article distributed under the terms and conditions of the Creative Commons Attribution (CC BY) license (<https://creativecommons.org/licenses/by/4.0/>).

1. Introduction

Power semiconductors have been extensively studied as essential components of various power conversion devices for a long time. Among them, research has been focused on silicon (Si)-based power semiconductors, which are applied in various fields to enhance the efficiency and power density of power conversion devices. However, due to the physical limitations of Si-based power semiconductors, research efforts are actively pursuing new components that can overcome these limitations. Recently, there has been an increasing demand for GaN HEMTs, which possess wide-bandgap (WBG) characteristics, among power semiconductors [1].

GaN HEMT generates a two-dimensional electron gas (2DEG) structure based on the heterojunction of AlGaN and GaN. This results in high charge mobility and density, as well as reduced parasitic capacitance within the device, leading to advantages such as high-speed switching and low switching losses compared to Si power semiconductors. Therefore, the application of GaN HEMT in power conversion devices effectively enhances device efficiency and power density. However, the high-speed switching characteristics of GaN HEMTs can pose significant drawbacks in terms of systems with short-circuit and overcurrent aspects. GaN HEMTs typically have very low gate–source threshold voltages, making them susceptible to faulty turn-on due to high dv/dt and di/dt resulting from high-speed switching, thereby increasing the risk of short-circuit occurrence. The short-circuit performance of GaN HEMTs has been evaluated in [2], and although the duration varies depending on the applied voltage magnitude, the short-circuit withstand time of GaN HEMTs is very low on the order of hundreds of nanoseconds. Additionally, GaN-based power semiconductors have much smaller package sizes compared to conventional Si power semiconductors, which provides an advantage in terms of power density. However, due to the difficulty in dissipating heat through the package in the event of a short circuit, it is necessary to protect the device from short-circuit situations before critical failures or permanent performance degradation can occur.

Various power semiconductors with short-circuit withstand times can be seen in Figure 1. Examining the short-circuit withstand times tested up to a DC bus voltage of 400 V, E-mode GaN HEMTs can withstand durations of 520 ns and 400 ns at 350 V and 400 V conditions, respectively.

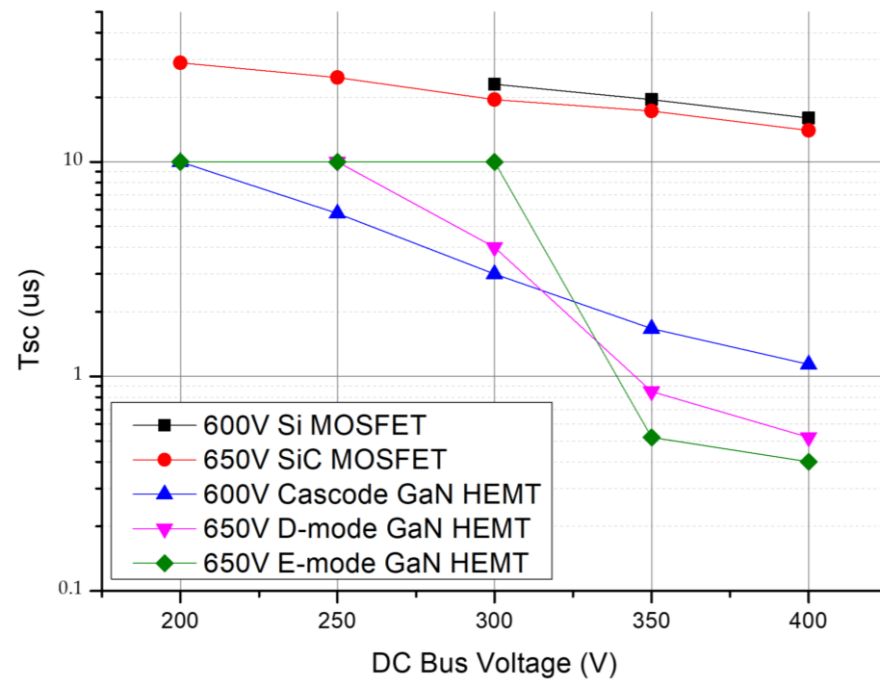


Figure 1. Short-circuit withstand times with voltage at 600 V/650 V for power semiconductors [3–6].

Additionally, at DC bus voltages below 350 V, E-mode GaN HEMTs exhibit relatively superior short-circuit endurance times ($T_{SC} > 10 \mu\text{s}$). Cascode GaN HEMTs demonstrate shorter short-circuit withstand times compared to E-mode GaN HEMTs at voltages below 300 V. However, at voltages of 350 V and above, Cascode GaN HEMTs exhibit short-circuit withstand times in the range of 1~2 μs [3–6].

Therefore, for GaN-based power semiconductors, which require very fast short-circuit protection compared to Si-based power semiconductors, it is generally challenging to apply commercially available gate drivers with saturation protection functions that require response times of 1 μs or more. Therefore, several short-circuit detection and protection techniques applicable to GaN-based power semiconductors have been explored. Incorporating a Shunt Resistor into the power loop in series to detect short-circuit currents presents a simple and universally adaptable solution for all systems. This current sensing method necessitates high-precision resistors and swift ADCs to ensure signal accuracy and detection speed. Refs [7,8] demonstrate the application of Shunt Resistors for short-circuit detection and protection in systems employing SiC and GaN devices, with detection and protection times recorded at 150 ns and 60 ns, respectively. However, the primary disadvantage of using Shunt Resistors for current sensing lies in power loss; high currents in high-power systems can lead to significant power loss across the Shunt Resistors, and low-power systems might require larger resistors to maintain signal accuracy, thereby reducing efficiency in low-power applications. Additionally, incorporating Shunt Resistors can increase parasitic inductance within the circuit, potentially affecting switching performance. Another method is to detect the high di/dt that occurs during a short circuit using the stray inductance inside the power semiconductor package. In [9–11], short-circuit protection is based on the stray inductance inside the SiC MOSFET package, and the times required for short-circuit detection and final protection are 60 ns, 140 ns and 1 μs , respectively. Although this approach can be used to achieve fast short-circuit protection, it requires a device with a Kelvin source to use the internal stray inductance

and requires the measurement of the internal stray inductance. In addition, unlike the SiC used in the reference, GaN devices have very small packages and have an internal stray inductance close to zero, making it difficult to apply the method even if a Kelvin source is present. Another short-circuit protection method is the use of Rogowski coils. In [12,13], a PCB-based auxiliary Rogowski coil is used to implement short circuit and overcurrent protection by di/dt measurements. The time required for the final protection is about 700 ns [12]. The method using a Rogowski coil allows fast operation by directly measuring the current, but the Rogowski coil current sensor requires an integrator circuit, making the circuit and implementation complex, and an output offset voltage is also generated due to the operational amplifier characteristics of the integrator circuit. In addition, the Rogowski coil has to be shielded as switching noise affects the current measurement. To detect overcurrent situations, refs. [14,15] utilize a portion of the power loop inductance. This is achieved by optimizing the PCB layout and reducing detection loss. The time required for short-circuit protection using this method is approximately 370 ns and 250 ns, respectively. The power loop inductance is implemented using PCB traces to minimize volume impact. When a high rate of change in the current is applied to the circuit due to a short circuit, the voltage induced in the power loop inductance exceeds a preset threshold, resulting in protective action. However, the practicality of this method is limited due to the inability to directly detect the current amplitude and voltage variability induced in the coil under different short-circuit conditions [16]. Another commonly used method is desaturation protection, which senses the drain-to-source voltage of a device. Desaturation protection can be easily implemented using commercially available gate driver devices. Refs. [17,18] utilized desaturation protection to achieve protection within 360 ns and 125 ns. However, this desaturation protection method was delayed due to the blanking time to avoid failure [19], and the additional diodes added capacitive load in parallel with the output capacitance on the power semiconductor, increasing switching losses [20]. Furthermore, the temperature dependence of $R_{ds,on}$ makes it challenging to define reference levels for desaturation protection [21]. Recently, research has been conducted on short circuit detection methods based on the DC bus voltage drop. In [6,22,23], short-circuit protection is performed based on the DC bus voltage, which is the voltage across the high-side device drain and low-side device source. The DC bus voltage exhibits an instantaneous voltage drop when a short circuit occurs because a high di/dt current flows through parasitic inductances present in the power loop. This voltage drop is used to detect whether a short circuit has occurred, and the response time of the detection circuit can be within hundreds of nanoseconds. In [22,23], the circuit is protected from a short circuit within 280 ns and 370 ns, respectively. However, when using DC bus voltage sensing, the voltage dip caused by the normal switching of the device can result in false short-circuit protection behavior.

In this paper, short circuits are detected by monitoring instantaneous drops in the DC bus voltage. In addition, a method is proposed that uses a bandpass filter to distinguish between voltage drops that occur during normal switching and short circuits. Section 2 of this paper explains the instantaneous voltage drop that occurs during a short circuit due to parasitic inductance in the circuit. Additionally, a bandpass filter is introduced to distinguish this from similar voltage drops that occur during normal switching. All analyses are performed based on PSPICE simulations.

Section 3 presents a short-circuit detection and protection circuit by applying the content covered in Section 2, and the operation of the circuit is confirmed through the PSPICE simulation. Experimental results with the proposed circuit are presented in Section 4. Section 5 concludes the paper.

2. Short Circuit Detection Method Based on DC Bus Voltage Drop

A half-bridge structure circuit is commonly used in power converters and has the structure shown in Figure 2. Among the components constituting the circuit, the DC-Link Capacitor serves to balance the instantaneous power difference between the input power and output load and minimize the voltage change in the DC-Link, and electrolytic capaci-

tors with relatively large capacitance are mainly used. Additionally, filter capacitors are placed near power semiconductors and DC-Link Capacitors to minimize the stray inductance components in the power loop. Ceramic capacitors with excellent high-frequency characteristics are preferred for this purpose.

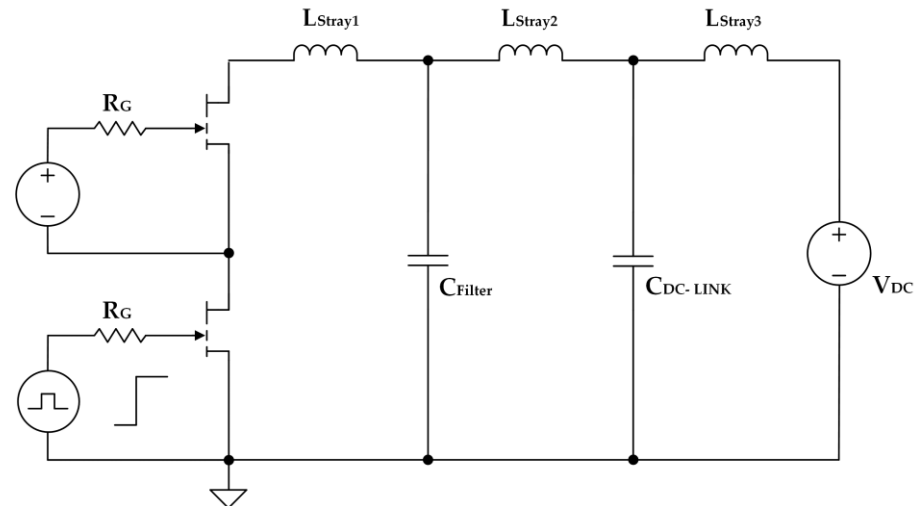


Figure 2. Short-circuit test circuit based on GaN HEMTs.

Stray inductance components denoted as L_{Stray} , are mostly formed by the PCB layout and can interfere with the stable operation of high-speed-switching GaN devices. Consequently, various research efforts are underway to minimize these components to ensure reliable operation. Despite these stray inductance components inevitably disrupting normal system operation, they can be effectively utilized to detect short circuits within the circuit.

2.1. Instantaneous Voltage Drop Due to Short Circuit

To measure the drop in the DC bus voltage during a short circuit, it is crucial to minimize the influence of stray inductance. This can be achieved by measuring the high-side device drain and low-side device source sides, as depicted in Figure 3a. Under normal switching conditions, as shown in Figure 3b, the DC bus voltage remains equal to the input voltage V_{DC} . However, during the occurrence of a short circuit, an instantaneous large di/dt current flows through the half-bridge, resulting in an instantaneous voltage drop in the DC bus voltage, as illustrated in Figure 3c, due to the circuit's stray inductance. The amplitude of this voltage drop is proportional to the voltage across L_{Stray1} , which is equal to Equation (1), and the stray inductance in the circuit is determined during PCB fabrication, so the amplitude of the voltage drop is determined by di/dt .

$$V_{L_stray1} = L_{\text{Stray1}} \frac{di}{dt} \quad (1)$$

The slope at the time of a short circuit is determined by the switch's turn-on time, which depends on the gate resistance value. Therefore, when detecting a short circuit through a drop in the DC bus voltage, it is essential to consider the gate resistance value used in the circuit. Although some power semiconductor datasheets may provide a correlation between the gate resistance value and switching time, this information is not available for the GS-065-011-1-L from GaNsystem used in this paper. Therefore, the SPICE model provided by the manufacturer can be used to determine the main phenomena that occur during a short circuit. Therefore, in this paper, an LTSPICE-based simulation circuit was constructed using the SPICE model of the device, as shown in Figure 4. Then, an analysis was performed on the instantaneous voltage drop that appears in the DC bus voltage [24].

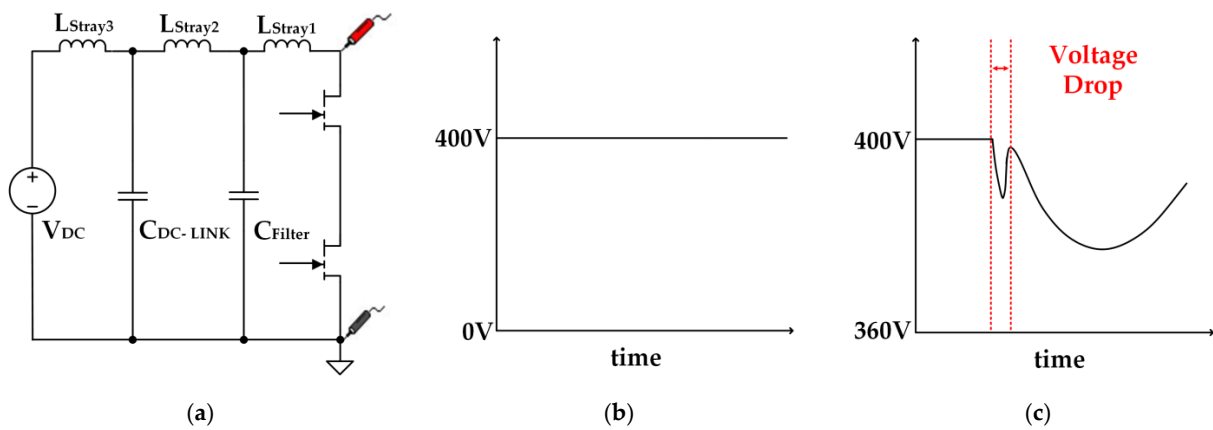


Figure 3. DC bus voltage-based short-circuit detection method (a) detection point. (b) DC bus voltage waveform during normal operation. (c) DC bus voltage waveform when a short circuit occurs.

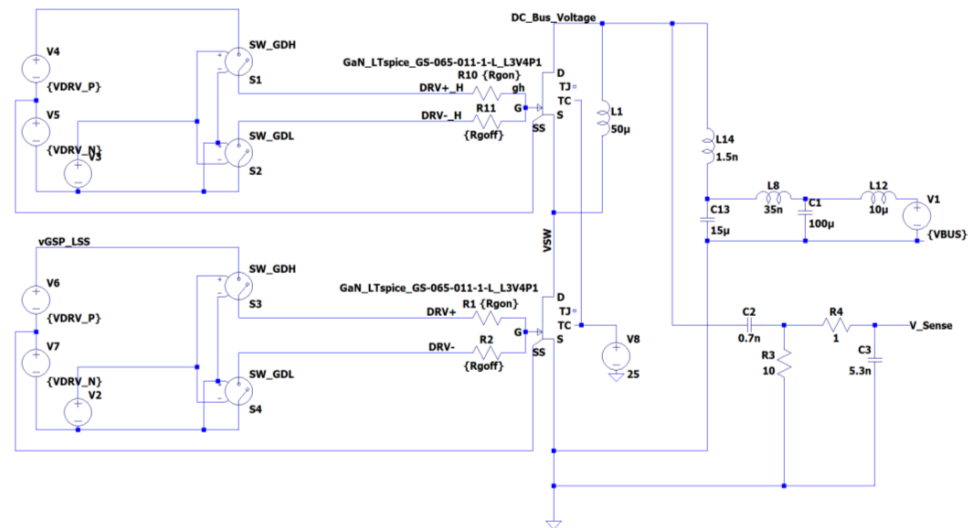


Figure 4. Simulation circuit diagram based on LT spice.

First, a simulation was performed to determine the instantaneous drop in DC bus voltage that occurs in a short circuit situation. Figure 4 shows the circuit used in the simulation, where the high-side GaN HEMT is always on, and the low-side GaN HEMT turns on 20 ns after the start of the simulation. There may be differences in simulation results depending on the presence or absence of parasitic resistance components present in the circuit. However, because the parasitic resistance components present in the PCB pattern and DC power connection line are sufficiently small, they do not have a significant impact on the simulation results. Therefore, the resistance component was not considered in the simulation. Additionally, because the size of the capacitor in the circuit was sufficiently large, changes in stray inductance components except L_{Stray1} did not affect the DC bus voltage drop. Therefore, in the simulation, the voltage drop level of the DC bus voltage was checked by changing the values of L_{Stray1} and C_{Filter} , which are key components that directly affect the instantaneous drop in the DC bus voltage.

Table 1 displays the main parameters used in the simulation, and Figure 5 shows the results. Figure 5a illustrates the effect of changing the value of L_{Stray1} , the stray inductance between the filter capacitor and the half-bridge in the circuit, on the voltage drop, and it can be seen that the value of L_{Stray1} directly affects the magnitude of the voltage drop that occurs at the moment of the short circuit, and the larger the value of L_{Stray1} , the larger the amplitude of the voltage drop. Figure 5b shows the voltage drop waveform at the short circuit according to the value of the filter capacitor, and it can be seen that the value of the

filter capacitor does not affect the magnitude of the voltage drop at the short circuit, but it does affect the magnitude of the voltage in the saturation region after the instantaneous voltage drop.

Table 1. Simulation parameter.

	L_{Stray1}	L_{Stray2}	C_{Filter}	$C_{DC-Link}$
Value	0.2 nH 0.5 nH 1 nH 1.5 nH	35 nH	0.2 μ F 0.5 μ F 1 μ F 1.5 μ F	100 μ F

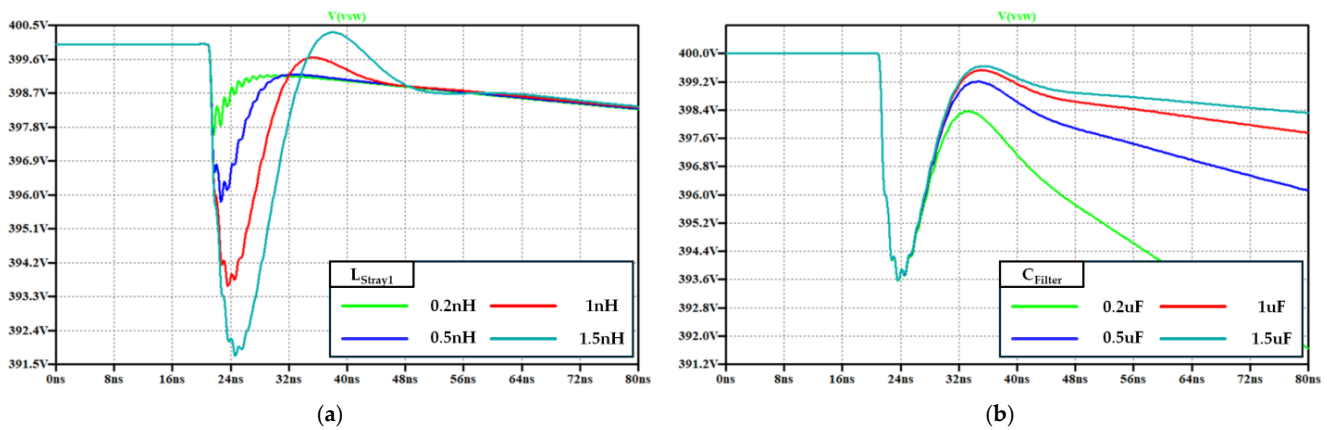


Figure 5. Simulation results of DC bus voltage drop by parameter changes in (a) stray inductance (L_{Stray1}). (b) Filter capacitor (C_{Filter}).

The simulation results show that the value of L_{Stray1} and the gate resistors present in the circuit have a significant impact on the instantaneous voltage drop of the DC bus voltage used in the short-circuit protection circuit. In PCB design, the value of L_{Stray1} typically ranges from a few to tens of nanoHenrys. Additionally, the gate resistor is selected based on factors such as the dv/dt , di/dt , and EMI of the circuit. Depending on the values of these factors, an instantaneous drop in the DC bus voltage is expected to provide meaningful results for short-circuit detection. Figure 6 illustrates the amplitude of the DC bus voltage drop as a function of gate resistance and the L_{Stray1} value when the input voltage is 400 V.

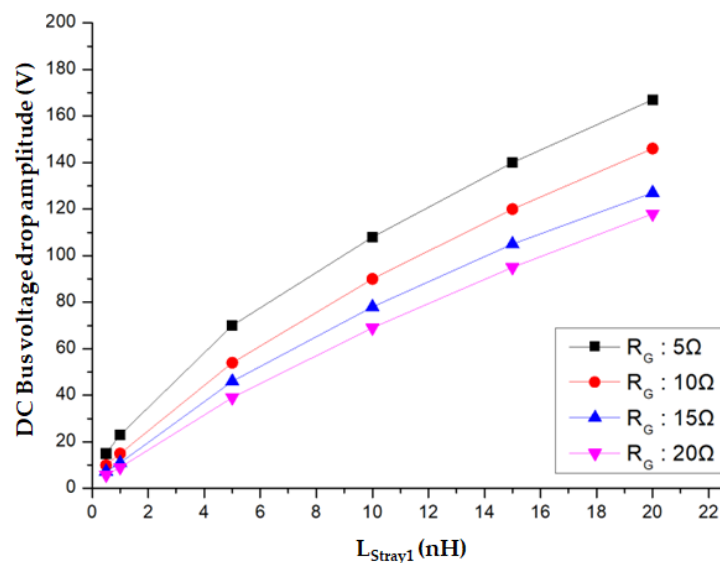


Figure 6. DC bus voltage drops depending on gate resistance and L_{Stray1} .

2.2. Instantaneous Voltage Drop Due to Normal Switching

However, the instantaneous voltage drop in the DC bus voltage does not only occur during short-circuit conditions. Figure 7a illustrates the situation when the power semiconductor device under test (DUT) is turned on during a typical double pulse test. At this point, the current flows through the load inductor to form the test current waveform. Figure 7b illustrates that when the DUT is turned on while the upper device is already on, the short circuit current flows through both the upper and lower devices, causing an instantaneous voltage drop similar to that observed earlier. Figure 8 shows the simulation results of implementing a typical double pulse test, observing the DC bus voltage at the moment the low-side device turns on. Similar to the voltage drop observed during a short circuit, a voltage drop is also identified during normal switching operations. It is important to differentiate between the voltage drop in the DC bus voltage that occurs during normal switching and that which occurs during a short circuit.

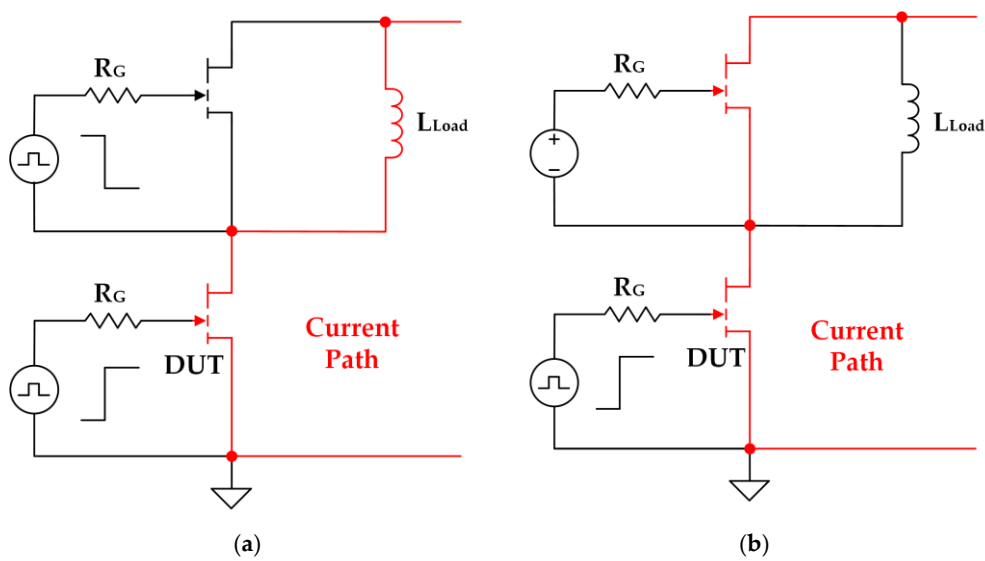


Figure 7. Current path when DC bus voltage drops: (a) double pulse test; (b) short circuit situation.

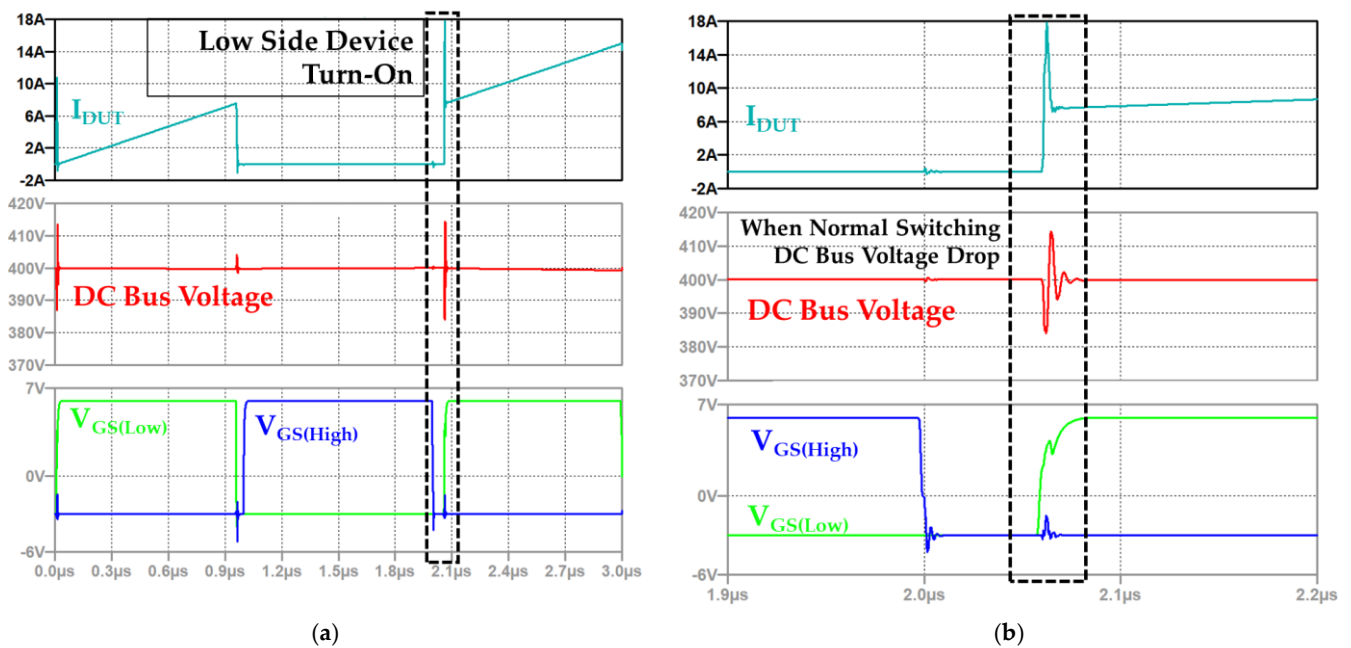


Figure 8. Double pulse tests waveforms: (a) full waveform; (b) zoomed waveform.

Figure 9a shows the voltage drops observed by SPICE simulations during switching and short-circuiting events. It can be seen that the voltage drop during a short-circuit condition is of a higher magnitude compared to the voltage drop during a switching condition. Bandpass filtering can be used to distinguish between these two voltage drops. Figure 9b presents the FFT analysis of the DC bus voltage during switching and short circuit events. Since the difference between the two voltages is greatest in the 20~30 MHz frequency range, the voltage drops can be distinguished by selecting the appropriate frequency band as the bandwidth using a bandpass filter. Therefore, the bandpass filter is designed to pass this frequency range. Figure 10 shows the schematic of the proposed bandpass filter, which consists of components C_1 , R_1 , C_2 , and R_2 .

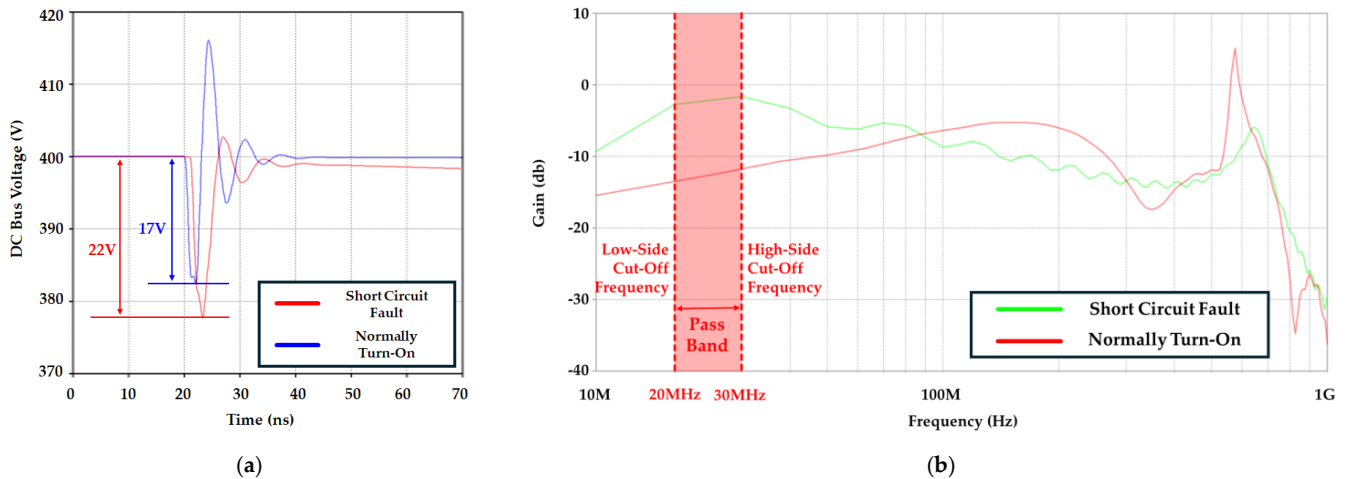


Figure 9. Comparison of switching and short circuit events (a) DC bus voltage drop; (b) fast Fourier transform (FFT).

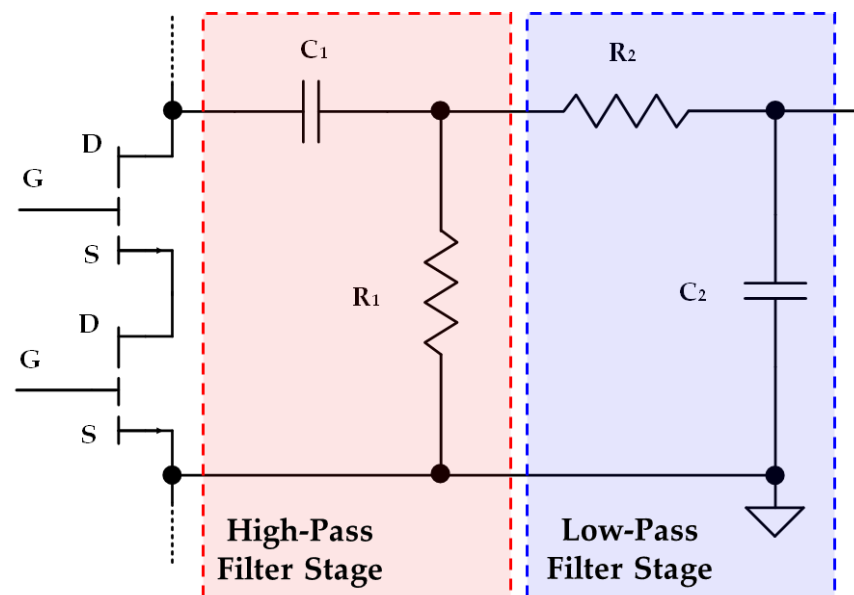


Figure 10. Bandpass filter for short circuit signal detection.

The bandpass filter is composed of a combination of low-pass and high-pass filters, which are utilized to detect voltage drop signals while blocking the DC voltage and high-frequency switching noise. As shown in Figure 10, the first stage of the circuit consists of a passive RC high-pass filter. This filter allows signals with frequencies above the low cutoff

frequency (f_{c-low}) to pass while attenuating signals with frequencies below f_{c-low} . The low cutoff frequency is given by Equation (2).

$$f_{c-low} = \frac{1}{2\pi R_1 C_1} \quad (2)$$

The second stage of the circuit is a passive RC low-pass filter. This filter allows signals with frequencies below the high cutoff frequency (f_{c-high}) to pass while attenuating signals with frequencies above f_{c-high} . The high cutoff frequency is calculated using Equation (3).

$$f_{c-high} = \frac{1}{2\pi R_2 C_2} \quad (3)$$

The specific frequency range through which a bandpass filter allows signals to pass is called the bandwidth. The bandwidth is calculated as the difference between the high and low cutoff frequencies, as described by Equation (4).

$$\text{Bandwidth} = f_{c-high} - f_{c-low} \quad (4)$$

In Figure 9b, the high-pass frequency is set to 20 MHz, and the low-pass frequency is set to 30 MHz, resulting in a bandwidth of 10 MHz. As can be seen from Equations (2) and (3), there are infinite combinations of resistors and capacitors that can satisfy the relevant frequency. Therefore, among the combinations that can satisfy the corresponding frequency, C_1 : 790 pF, R_1 : 10 Ω , R_2 : 1 Ω and C_2 : 5.3 nF were promoted. However, to apply this value, since there were no exact matching values among commercial products, resistors and capacitors with the closest values among commercial products were used. The filter element values of the final bandpass filter used were C_1 : 750 pF, R_1 : 10 Ω , R_2 : 1 Ω and C_2 : 5.1 nF. Therefore, the actual applied high-pass frequency was 21 MHz, and the low-pass frequency was 31 MHz.

3. Proposed Short-Circuit Protection Circuit

This section presents a proposed fast protection method based on DC bus voltage detection using the proposed detection signal and detection circuit, as shown in Figure 11. The voltage detected in the detection circuit is transferred to the input of the comparator. When a short circuit occurs, a voltage drop in the DC bus voltage is detected, which triggers the detection signal in the comparator. Since the voltage drop in the DC bus voltage that occurs during a short circuit is transient, a logic control circuit such as an SR latch can be used, as shown in Figure 11. Finally, the generated error signal is applied to the disable pin of the gate driver to disable it.

To verify the proper operation of the proposed circuit, SPICE-based simulations were performed to simulate normal switching and fault conditions and confirm the fault signal detection and protection actions. Figure 12 shows the simulation results using the double-pulse test circuit, where the switching instance of the DC bus voltage and the occurrence of the fault signal are observed. At approximately 2.05 μ s, the low-side device was turned on, resulting in an instantaneous voltage drop in the DC bus voltage. However, the fault signal detected by the sensing circuit, shown as V_{Sense} , only dropped to -1.8 V and did not fall below the -2 V threshold. Consequently, the signal required to disable the gate driver was not generated.

Figure 13 shows the waveform that confirms the DC bus voltage and short-circuit signal generation during a short circuit using the same circuit. Since the high-side device is always turned on, a short circuit occurs at 20 ns when the low-side device turns on. At this time, an instantaneous voltage drop in the DC bus voltage and the short-circuit signal V_{Sense} detected by the short-circuit detection circuit drops below the -2 V threshold. The short-circuit signal finally generates a protective operation signal through the comparator, and the signal is formed 93 ns after the short-circuit occurs and is applied to the gate driver's disable pin to protect the circuit from short-circuit.

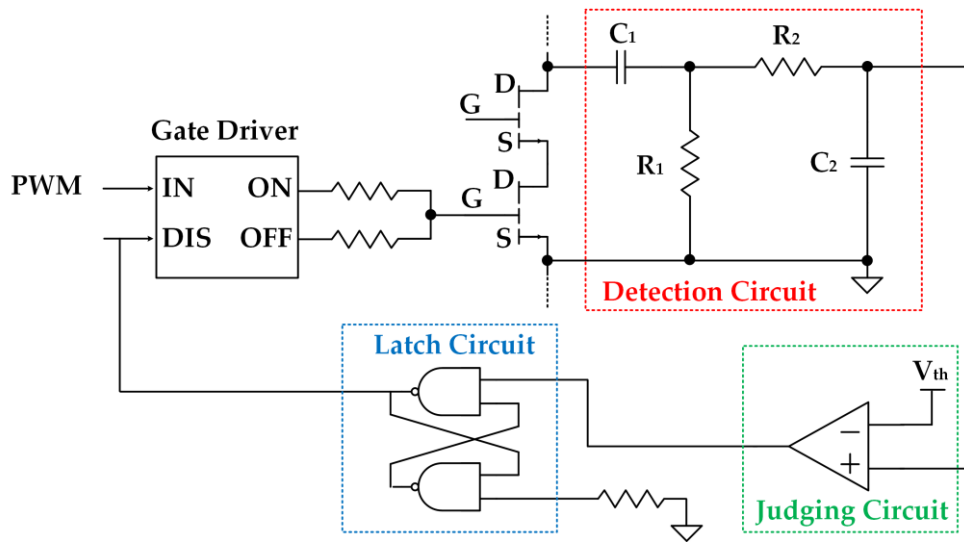


Figure 11. Proposed short-circuit protection circuit.

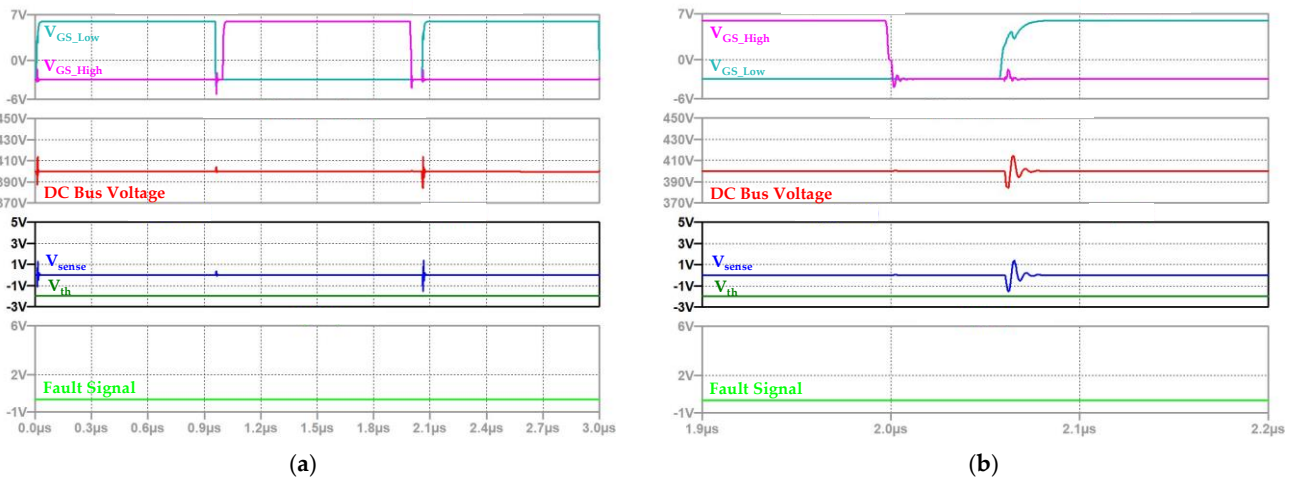


Figure 12. Simulation waveforms during switching (a) full waveforms. (b) Zoomed waveforms.

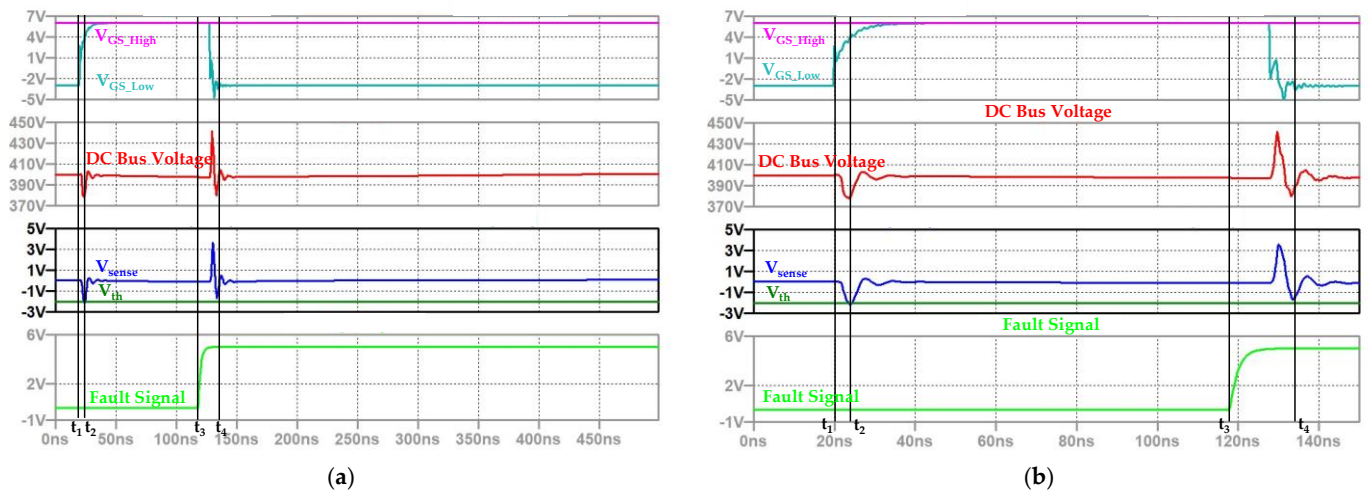


Figure 13. Short circuit simulation waveform (a) full waveform. (b) Zoomed waveform.

The simulation results show that when a short-circuit occurs in a circuit using GaN HEMT, the protection based on the short-circuit detection circuit proposed in this paper is

performed correctly. The simulation waveform shows that the final signal for short-circuit protection is formed 93 ns after the short-circuit occurs, and it takes only 105 ns to turn off the GaN HEMT. The proposed circuit is more efficient in protecting against short circuits than the existing desaturation method, as it requires a much shorter time for short-circuit protection.

4. Experimental Results

To verify the feasibility of our proposed circuit, a test board was fabricated like the circuit in Figure 14 using the same structure as in the simulation. The test board used in the experiment is shown in Figure 15a, and the complete test bed setup is shown in Figure 15b. The parameters used in the experiment are detailed in Table 2. The test bed enables the execution of double pulse and short circuit tests, and the GaN system’s GS-065-011-1-L device is used for the experiment. The experiment was carried out at an ambient temperature of 25 °C.

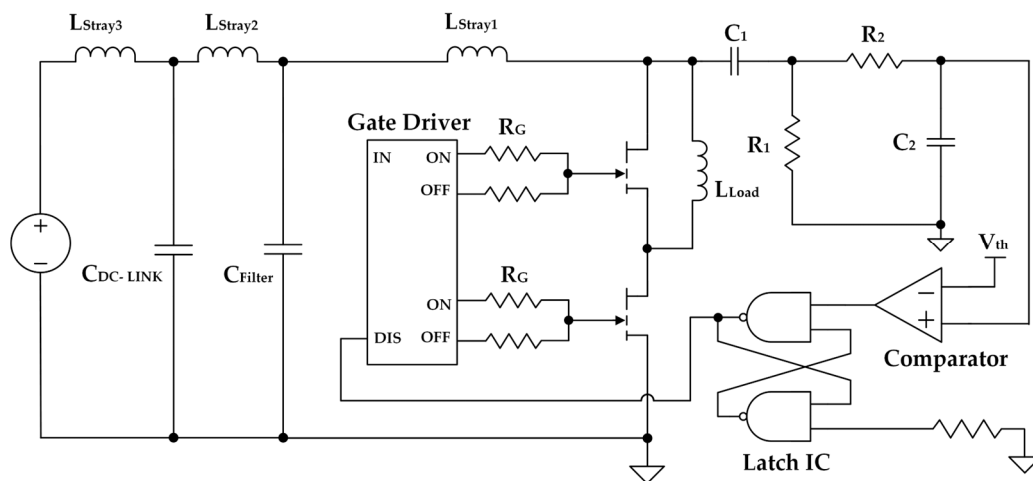
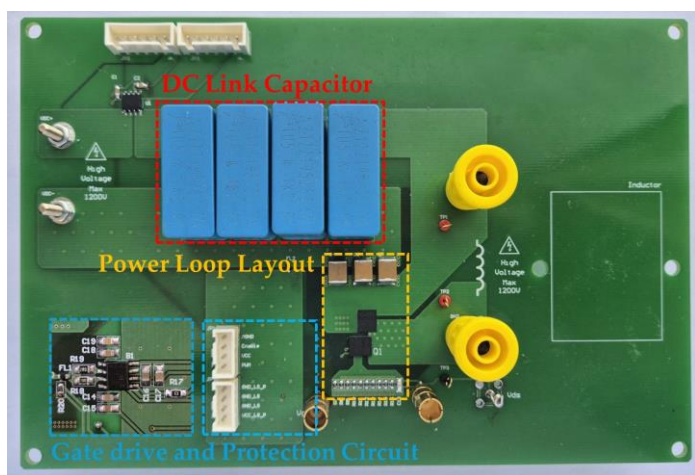
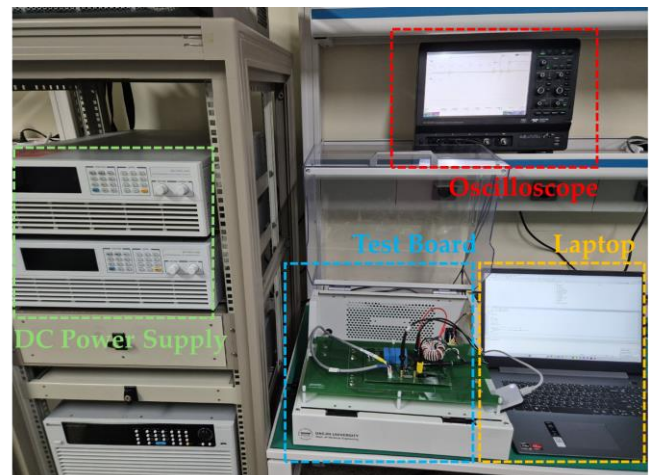


Figure 14. Circuit diagram of the board used in the experiment.



(a)



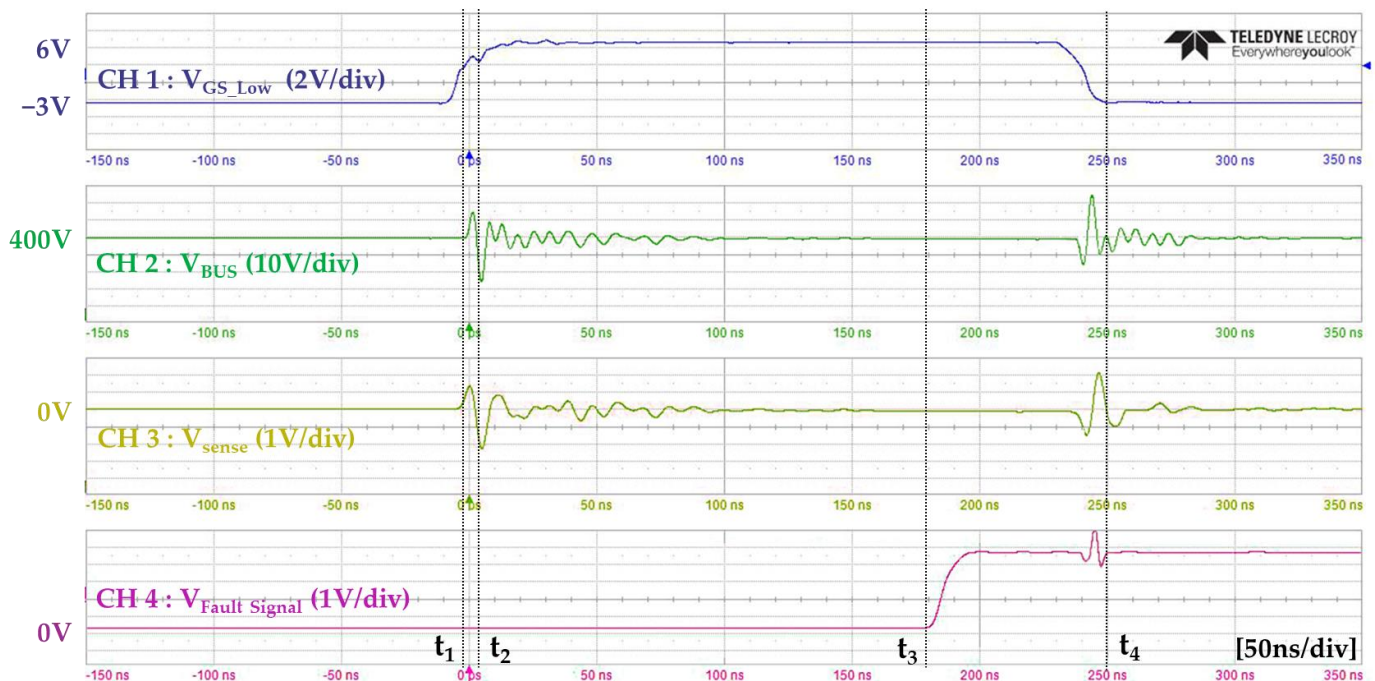
(b)

Figure 15. Experimental setup: (a) test board. (b) Test setup.

Table 2. Experimental parameter.

Parameter	$C_{DC-Link}$	C_{Filter}	L_{Stray1}	L_{Stray1}
Value	100 μ F	4 μ F	1.5 nH	35 nH
Parameter	V_{DC}	L_{Load}	R_{G_ON}	V_{On}/V_{Off}
Value	400 V	100 μ H	15 Ω	6 V / -3 V
Parameter	R_1	C_1	R_2	C_2
Value	10 Ω	750 pF	1 Ω	5.1 nF

Figure 16 shows the protective operation of the proposed circuit. Channel 1 (CH 1) represents the gate–source voltage of the low-side GaN HEMT, while Channel 2 (CH 2) represents the DC bus voltage. Channel 3 (CH 3) is the output signal of the bandpass filter, which detects voltage drops, and Channel 4 (CH 4) represents the fault signal applied to the disable pin of the gate driver.

**Figure 16.** Experimental waveforms when a short circuit occurs.

As the gate voltage of the low-side GaN HEMT, corresponding to CH 1 in Figure 16 rises from -3 V to 6 V, the low-side device turns on. At point t_1 , when the low-side gate–source voltage exceeds the device’s threshold voltage, the short-circuit current begins to flow, and distortion occurs in the DC bus voltage. At time t_2 , the instantaneous voltage drop in the DC bus voltage corresponding to CH 2 appears the largest. At this time, there is a voltage drop of 25 V from 400 V to 375 V. This voltage drop passes through a bandpass filter and appears on CH 3. The output of the bandpass filter maintains V_{Sense} at 0 V in a normal condition. However, when a short circuit occurs, the voltage shows an instantaneous drop similar to the DC bus voltage, decreasing to -2.2 V at time t_2 . This is 10 ns after the device is turned on and the short circuit occurs. Since the magnitude of the voltage V_{th} applied to the negative pin of the comparator is -2 V, a fault signal is formed through the output of the comparator when V_{Sense} becomes less than V_{th} . The fault signal is initially generated from the comparator output, proceeds through the latch circuit to maintain the high signal and is then applied to the gate driver’s disable pin. It appears in fault signal CH 4 and rises from 0 V to 5 V after 177 ns from t_2 , and the delay that appears between t_2 and t_3 is caused by the propagation

delay of the comparator and latch IC. After the fault signal is applied to the disable pin of the gate driver, about 50 ns later, the low-side gate source voltage of CH 1 begins to decrease. It takes about 20 ns, and the device is completely turned off at time t_4 . Therefore, it can be confirmed that the device is completely turned off a total of 257 ns after the short circuit occurs, thereby protecting the circuit.

Since it has been confirmed that the proposed short-circuit protection circuit operates normally during a short circuit, it has been confirmed that the short-circuit protection circuit does not operate during normal switching operations. The experiment can be seen in Figure 17. Figure 17 is an enlarged waveform of the moment when the second pulse is applied during the double pulse test operation. CH 1 represents the gate–source voltage of the low-side GaN HEMT, CH 2 represents the DC bus voltage, CH 3 represents the voltage drop detection signal, and CH 4 represents the fault signal. At time t_1 , the gate–source voltage of the low-side GaN HEMT exceeds the threshold, causing distortion of the DC bus voltage. At t_2 , the DC bus voltage drop reaches its maximum, and the voltage, which is maintained at 400 V in the normal state, decreases by 22 V to 378 V. The V_{Sense} voltage of CH 3 shows a similar form to the DC bus voltage and has the lowest value at time t_2 , but it can be seen that it is greatly attenuated after passing through the bandpass filter. In the normal state, the voltage is maintained at 0 V but decreases to -1 V at time t_2 . The V_{Sense} voltage is applied to the positive pin of the comparator and does not become less than -2 V, which is the voltage being applied to the negative pin. Therefore, the output of the comparator continues to remain at 0 V and no fault signal is formed.

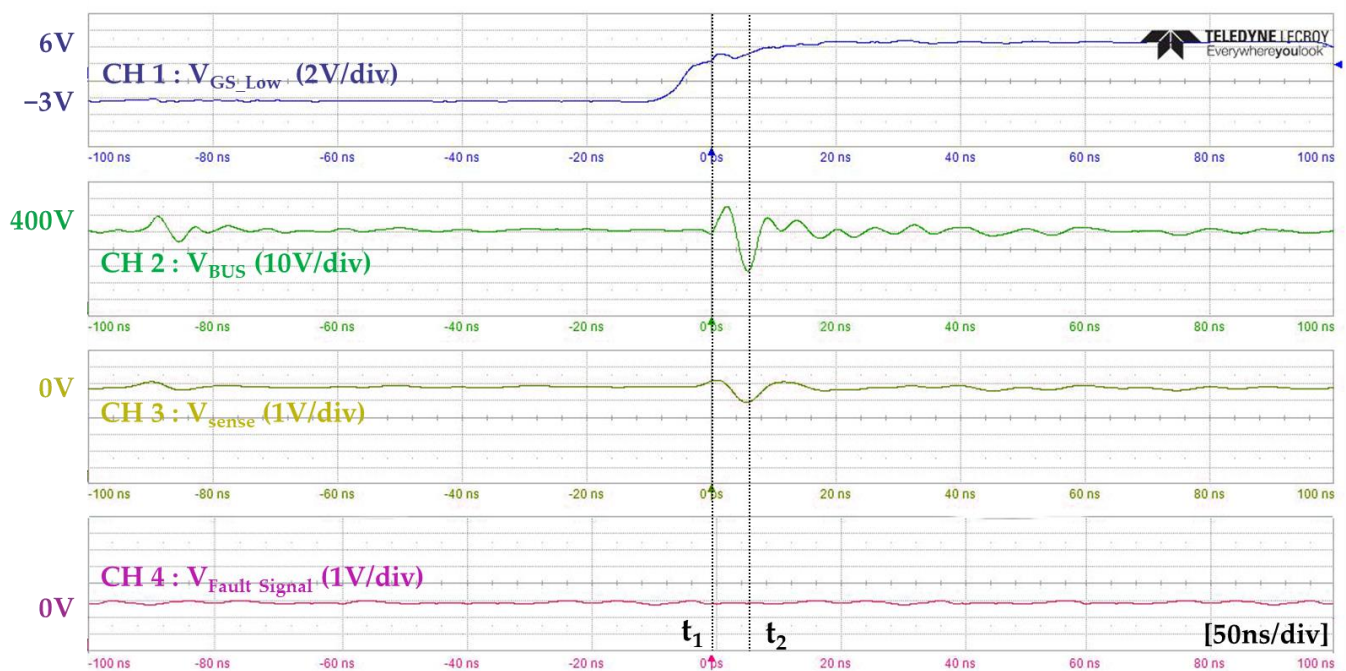


Figure 17. Experimental waveforms during normal switching.

During a short circuit, the DC bus voltage drops by 25 V, while during normal switching (turn-on), the voltage drop is 22 V, which is larger during a short circuit. However, after passing through a bandpass filter, the voltage drop decreases to 2.2 V during a short circuit and 1 V during normal switching. As such, it can be seen that there is a significant difference in the attenuation level of the DC bus voltage that appears as it passes through the bandpass. It is confirmed that the proposed circuit can distinguish between short-circuit and normal switching and effectively provide short-circuit protection.

Table 3 compares the proposed short-circuit protection method with an existing study related to short-circuit protection of wide-bandgap power semiconductors. In the existing study, various methods were applied to protect SiC and GaN-based power semiconductors,

and the time required for short-circuit protection was on the order of hundreds of ns. The proposed method did not have the fastest protection operation speed compared to the existing study. However, it had an above-average protection operation speed. And it can also be implemented with fewer elements compared to the average number of elements used. In addition, the proposed short-circuit protection method effectively prevents malfunctions during normal switching through a bandpass filter, achieving the high reliability of short-circuit protection operations.

Table 3. Comparison with existing studies.

Reference	Device	Protection Method	Component (Passive/Active)	Protection Time
[7]	SiC	Shunt Resistor	4/3	150 ns
[8]	GaN	Shunt Resistor	-	60 ns
[9]	SiC	Package Internal Inductance	5/4	60 ns
[10]	SiC	Package Internal Inductance	6/7	100 ns
[12]	SiC	Rogowski coil	4/5	700 ns
[13]	SiC	Rogowski coil	8/5	-
[14]	GaN	Stray inductance	-	250 ns
[15]	GaN	Stray inductance	3/5	250 ns
[17]	GaN	Desaturation	4/4	360 ns
[18]	GaN	Desaturation	8/5	125 ns
[22]	GaN	DC bus voltage	4/3	280 ns
[23]	GaN	DC bus voltage	8/5	370 ns
Proposed	GaN	DC bus voltage	5/2	257 ns

5. Conclusions

In this paper, a short-circuit detection and protection circuit for GaN HEMT is proposed and verified. GaN HEMT has a shorter short-circuit withstand time compared to other types of power semiconductors, so it requires a short-circuit protection circuit that has high reliability and operates at high speeds. The proposed short-circuit protection method uses a method of detecting the DC bus voltage for fast short-circuit protection. The high di/dt current that appears during a short circuit causes an instantaneous voltage drop in the parasitic inductance present in the circuit. Therefore, when a short circuit occurs, an instantaneous voltage drop occurs in the inductance component present in the power loop, and an instantaneous voltage drop also occurs in the DC bus voltage, which remains the same as the DC link voltage in the normal state. This DC bus voltage drop is a quick and clear indicator of the occurrence of a short circuit and can be used to effectively protect the circuit from short circuits. However, similar voltage drops can occur in normal switching situations as well. In the proposed short-circuit protection method, the frequency analysis of the DC bus voltage drop was performed based on the SPICE simulation. Based on that analysis, a bandpass filter was used to effectively distinguish between the two types of voltage drops. When using the proposed short-circuit protection method, short-circuit protection was finally completed 257 ns after the short-circuit occurred. In practice, after a short circuit occurs, it takes 10 ns for the output signal of the bandpass filter to be compared to the comparator threshold. Therefore, it is expected that short-circuit protection will be possible at a faster rate if the propagation delay of the comparator IC and latch IC used in the experiment is reduced. Future research should be conducted to improve the time required for short-circuit protection in the proposed method.

Author Contributions: Conceptualization, C.-M.K.; Methodology, C.-M.K.; Software, C.-M.K.; Validation, C.-M.K.; Formal analysis, C.-M.K. and N.-J.K.; Investigation, H.-S.Y.; Resources, N.-J.K.; Data curation, C.-M.K.; Writing—original draft, C.-M.K.; Writing—review and editing, J.-S.K. and N.-J.K.; Visualization, C.-M.K. and H.-S.Y.; Supervision, N.-J.K.; Project administration, N.-J.K. All authors have read and agreed to the published version of the manuscript.

Funding: This work was supported by the Ministry of Education of the Republic of Korea and the National Research Foundation of Korea (NRF-2021R1F1A10506811).

Data Availability Statement: The data are available in a publicly accessible repository.

Conflicts of Interest: The authors declare no conflicts of interest.

References

1. Lidow, A.; Strydom, J. *Gallium Nitride (GaN) Technology Overview*; White Paper; Efficient Power Conversion Corporation (EPC-co): El Segundo, CA, USA, 2012.
2. Li, H.; Li, X.; Wang, X.; Wang, J.; Alsmadi, Y.; Liu, L.; Bala, S. E-mode GaN HEMT short circuit robustness and degradation. In Proceedings of the 2017 IEEE Energy Conversion Congress and Exposition (ECCE), Cincinnati, OH, USA, 1–5 October 2017; pp. 1995–2002. [CrossRef]
3. Huang, X.; Lee, D.Y.; Bondarenko, V.; Baker, A.; Sheridan, D.C.; Huang, A.Q.; Baliga, B.J. Experimental study of 650V AlGaIn/GaN HEMT short-circuit safe operating area (SCSOA). In Proceedings of the IEEE International Symposium on Power Semiconductor Devices & IC's (ISPSD), Waikoloa, HI, USA, 15–19 June 2014; pp. 273–276.
4. Badawi, N.; Awwad, A.E.; Dieckerhoff, S. Robustness in short-circuit mode: Benchmarking of 600V GaN HEMTs with power Si and SiC MOSFETs. In Proceedings of the IEEE Energy Conversion Congress and Exposition (ECCE), Milwaukee, WI, USA, 18–22 September 2016; pp. 1–7.
5. Fernández, M.; Perpiñà, X.; Roig, J.; Vellvehi, M.; Bauwens, F.; Jordà, X.; Tack, M. P-GaN HEMTs Drain and Gate Current Analysis Under Short-Circuit. *IEEE Trans. Electron Device Lett.* **2017**, *38*, 505–508. [CrossRef]
6. Kim, C.-M.; Kim, J.-S.; Kim, N.-J. Study on GaN FET Short Circuit Characteristics and Development of Effective Short Circuit Protection Method. In Proceedings of the 2022 25th International Conference on Electrical Machines and Systems (ICEMS), Chiang Mai, Thailand, 29 November–2 December 2022; pp. 1–5.
7. Awwad, A.E.; Dieckerhoff, S. Short-circuit evaluation and overcurrent protection for SiC power MOSFETs. In Proceedings of the 2015 17th European Conference on Power Electronics and Applications (EPE'15 ECCE-Europe), Geneva, Switzerland, 8–10 September 2015; pp. 1–9.
8. Zhang, W.; Wang, F.; Zhang, Z.; Holzinger, B. Fast Wide-bandgap Device Overcurrent Protection with Direct Current Measurement. In Proceedings of the 2019 10th International Conference on Power Electronics and ECCE Asia (ICPE 2019–ECCE Asia), Busan, Republic of Korea, 27–30 May 2019; pp. 1–6. [CrossRef]
9. Xue, J.; Xin, Z.; Wang, H.; Loh, P.C.; Blaabjerg, F. An improved di/dt-RCD detection for short-circuit protection of SiC MOSFET. *IEEE Trans. Power Electron.* **2021**, *36*, 12–17. [CrossRef]
10. Wang, Z.; Shi, X.; Xue, Y.; Tolbert, L.M.; Wang, F.; Blalock, B.J. Design and performance evaluation of overcurrent protection schemes for Silicon Carbide (SiC) power MOSFETs. *IEEE Trans. Ind. Electron.* **2014**, *61*, 5570–5581. [CrossRef]
11. Sun, K.; Wang, J.; Burgos, R.; Boroyevich, D. Design, Analysis, and Discussion of Short Circuit and Overload Gate-Driver Dual-Protection Scheme for 1.2-kV, 400-A SiC MOSFET Modules. *IEEE Trans. Power Electron.* **2020**, *35*, 3054–3068. [CrossRef]
12. Stecca, M.; Tiftikidis, P.; Soeiro, T.B.; Bauer, P. Gate Driver Design for 1.2 kV SiC Module with PCB Integrated Rogowski Coil Protection Circuit. In Proceedings of the 2021 IEEE Energy Conversion Congress and Exposition (ECCE), Vancouver, BC, Canada, 10–14 October 2021; pp. 5723–5728. [CrossRef]
13. Rafiq, A.; Pramanick, S. Ultrafast Protection of Discrete SiC MOSFETs With PCB Coil-Based Current Sensors. *IEEE Trans. Power Electron.* **2023**, *38*, 1860–1870. [CrossRef]
14. Alemdar, O.S.; Karakaya, F.; Keysan, O. PCB Layout Based Short-Circuit Protection Scheme for GaN HEMTs. In Proceedings of the 2019 IEEE Energy Conversion Congress and Exposition (ECCE), Baltimore, MD, USA, 29 September–3 October 2019; pp. 2212–2218. [CrossRef]
15. Karakaya, F.; Alemdar, O.S.; Keysan, O. Layout-Based Ultrafast Short-Circuit Protection Technique for Parallel-Connected GaN HEMTs. *IEEE J. Emerg. Sel. Top. Power Electron.* **2021**, *9*, 6385–6395. [CrossRef]
16. Jiang, W.L.; Murray, S.K.; Zaman, M.S.; De Vleeschouwer, H.; Moens, P.; Roig, J.; Trescases, O. An Integrated GaN Overcurrent Protection Circuit for Power HEMTs Using SenseHEMT. *IEEE Trans. Power Electron.* **2022**, *37*, 9314–9324. [CrossRef]
17. Sadik, D.-P.; Colmenares, J.; Tolstoy, G.; Peftitsis, D.; Bakowski, M.; Rabkowski, J.; Nee, H.-P. Short-Circuit Protection Circuits for Silicon-Carbide Power Transistors. *IEEE Trans. Ind. Electron.* **2016**, *63*, 1995–2004. [CrossRef]
18. Hou, R.; Lu, J.; Chen, D. An Ultrafast Discrete Short-Circuit Protection Circuit for GaN HEMTs. In Proceedings of the 2018 IEEE Energy Conversion Congress and Exposition (ECCE), Portland, OR, USA, 23–27 September 2018; pp. 1920–1925. [CrossRef]
19. Acuna, J.; Walter, J.; Kalfass, I.; Gan, G.N. Very fast short circuit protection for gallium-nitride power transistors based on printed circuit board integrated current sensor. In Proceedings of the 2018 20th European Conference on Power Electronics and Applications (EPE'18 ECCE Europe), Riga, Latvia, 17–21 September 2018; pp. 1–10. Available online: <https://ieeexplore.ieee.org/document/8515547> (accessed on 13 January 2024).
20. Jones, E.A.; Williford, P.; Wang, F. A fast overcurrent protection scheme for GaN GITs. In Proceedings of the 2017 IEEE 5th Workshop on Wide-Bandgap Power Devices and Applications, Albuquerque, NM, USA, 30 October–1 November 2017; pp. 277–284.

21. Sun, K.; Wang, J.; Burgos, R.; Boroyevich, D.; Kang, Y.; Choi, E. Analysis and design of an overcurrent protection scheme based on parasitic inductance of SiC MOSFET power module. In Proceedings of the 2018 IEEE Applied Power Electronics Conference and Exposition (APEC), San Antonio, TX, USA, 4–8 March 2018; pp. 2806–2812.
22. Li, H.; Lyu, X.; Wang, K.; Abdullah, Y.; Hu, B.; Yang, Z.; Wang, J.; Liu, L.; Bala, S. An Ultra-Fast Short Circuit Protection Solution for E-mode GaN HEMTs. In Proceedings of the 2018 1st Workshop on Wide Bandgap Power Devices and Applications in Asia (WiPDA Asia), Xi'an, China, 17–19 May 2018; pp. 187–192. [[CrossRef](#)]
23. Zhou, Y.; Bai, Z.; Gong, X. Study of a Fast Over-Current Protection Based on Bus Voltage Drop for Gallium Nitride Power Device. *IOP Conf. Ser. Mater. Sci. Eng.* **2020**, *782*, 022085. [[CrossRef](#)]
24. Datasheet GS-065-011, GaN Systems. Available online: <https://gansystems.com/gan-transistors/gs-065-011-1-1/> (accessed on 13 January 2024).

Disclaimer/Publisher's Note: The statements, opinions and data contained in all publications are solely those of the individual author(s) and contributor(s) and not of MDPI and/or the editor(s). MDPI and/or the editor(s) disclaim responsibility for any injury to people or property resulting from any ideas, methods, instructions or products referred to in the content.